Monografías Matemáticas *García de Galdeano* **39**, 1–10 (2014)

DISCRETE HODGE HELMHOLTZ DECOMPOSITION

Etienne Ahusborde, Mejdi Azaïez, Jean-Paul Caltagirone, Mark Gerritsma and Antoine Lemoine

Abstract. This paper presents a new method using spectral approaches to compute the Discrete Hodge Helmholtz Decomposition (DHHD) of a given vector field. This decomposition consists in extracting the solenoidal (i.e. divergence-free), the non-solenoidal (i.e. rotational-free or, gradient of a scalar field) and the harmonic components (that is divergence-free and rotational-free) of a this vector field. A test case illustrates the proposed method.

Keywords: Discrete Hodge Helmholtz decomposition, spectral element method.

AMS classification: 76D05, 65N35.

§1. Introduction

The Hodge Helmholtz decomposition of a general vector field $\mathbf{u} = \mathbf{u}_\psi + \mathbf{u}_\phi + \mathbf{u}_H$ is a classical problem in applied and computational physics [11, 14]. Application areas include (among others) electromagnetism, linear elasticity, fluid mechanics, image and video processing. A closed form of this decomposition may be obtained for unbounded domains through Biot-Savart type integrals. In finite domains, however such an approach is no longer feasible and computational solutions are the only practical way to perform this decomposition.

With regard to elasticity, work by Brezzi and Fortin [7], and by Arnold and Falk [3] used the Hodge Helmholtz decomposition theorem for the study of the Reissner-Mindlin plate model. With regard to incompressible fluid flows, the scalar potential ϕ such that $\mathbf{u}_\phi = \nabla\phi$ in the Hodge Helmholtz decomposition is usually related to the pressure field p, and the vector potential $\mathbf{u}_\psi$ corresponds to the solenoidal velocity field $\mathbf{u}_S$ both quantities being involved in the Navier-Stokes equations [6]. Stokes and Navier-Stokes solvers decouple most of the time the computation of the velocity and pressure fields [10]. The family of correction-pressure time splitting methods [12] generates first a tentative velocity field that is not incompressible but contains the right vorticity. The addition of a pressure gradient to this temporary velocity (equivalent to Hodge Helmholtz decomposition) makes it divergence-free [9, 19]. Another approach resorts to pressure penalization [8]. In video processing, the Hodge Helmholtz decomposition allows to detect the fingerprint reference or hurricanes from satellite pictures [16]. In [1] the authors propose a constructive spectral approaches for the Helmholtz decomposition of a Vector Field which consists in projecting the field to be decomposed on the kernel and the ranges of the $-$ grad(div) operator. Recently, in [17], the authors proposed a meshless approach for the Hodge Helmholtz decomposition while in [13], divergence-free and curl-free wavelets are used.

§2. Discrete Hodge Helmholtz Decomposition

Consider a *given* vector field $\mathbf{u}$ defined in some domain Ω with boundary $\partial\Omega$. The Helmholtz decomposition writes (see [11, Theorem 3.2, p. 40])

$$\mathbf{u} = \mathbf{u}_\psi + \mathbf{u}_\phi + \mathbf{u}_H. \tag{1}$$

The solenoidal component $\mathbf{u}_\psi$ satisfies the equations

$$\begin{cases} \nabla \cdot \mathbf{u}_\psi = 0 \text{ in } \Omega, \\ \mathbf{u}_\psi \cdot \mathbf{n} = 0 \text{ on } \partial\Omega, \end{cases} \tag{2}$$

while the irrotational complement $\mathbf{u}_\phi$ is such that

$$\begin{cases} \nabla \times \mathbf{u}_\phi = \mathbf{0} \text{ in } \Omega, \\ \mathbf{u}_\phi \times \mathbf{n} = \mathbf{0} \text{ on } \partial\Omega. \end{cases} \tag{3}$$

Finally, the harmonic component is both solenoidal and irrotational:

$$\nabla \cdot \mathbf{u}_H = 0 \quad \text{and} \quad \nabla \times \mathbf{u}_H = \mathbf{0}. \tag{4}$$

The main difficulty of the problem (1) consists in satisfying the solenoidal (2) and irrotational constraints (3). The method we present in this paper is based on the construction of a basis satisfying the expected constraints. Its originality lies in the way these bases are built. To illustrate this, we will focus our presentation on how we derive a divergence-free basis. The derivation of the rotational-free basis in 2D will be presented in Section 4. This paper only considers the 2D case and then it is good to distinguish between curl and rot, where

$$\nabla \times \mathbf{u} = \operatorname{rot} \mathbf{u} = \frac{\partial u_2}{\partial x_1} - \frac{\partial u_1}{\partial x_2}, \quad \operatorname{curl} \phi = \begin{pmatrix} \partial\phi/\partial x_2 \\ -\partial\phi/\partial x_1 \end{pmatrix}.$$

§3. Computation of the solenoidal component

In order to state the problem in variational form we introduce the relevant spaces of functions:

$$H(\operatorname{div}, \Omega) = \left\{ \mathbf{w} \in (L^2(\Omega))^2 \;\middle|\; \nabla \cdot \mathbf{w} \in L^2(\Omega) \right\},$$
$$L^2_0(\Omega) = \left\{ q \in L^2(\Omega) \;\middle|\; \int_\Omega q \, dx = 0 \right\}.$$

Let $\mathbf{v}, \mathbf{w} \in H(\operatorname{div}, \Omega)$. We define the inner product

$$(\mathbf{v}, \mathbf{w})_{H(\operatorname{div},\Omega)} = (\mathbf{v}, \mathbf{w})_{(L^2(\Omega))^2} + (\nabla \cdot \mathbf{v}, \nabla \cdot \mathbf{w})_{L^2(\Omega)}, \tag{5}$$

and associated norm $\|\mathbf{w}\|_{H(\operatorname{div},\Omega)} = \left(\|\mathbf{w}\|^2_{(L^2(\Omega))^2} + \|\nabla \cdot \mathbf{w}\|^2_{L^2(\Omega)} \right)^{1/2}$.

Consider also the proper subspace $H_0(\operatorname{div}, \Omega) \subset H(\operatorname{div}, \Omega)$:

$$H_0(\operatorname{div}, \Omega) = \{ \mathbf{w} \in H(\operatorname{div}, \Omega) \mid \mathbf{w} \cdot \mathbf{n} = 0 \text{ on } \partial\Omega \}.$$

The admissible space for $\mathbf{u}_\psi$ in Problem (1)–(4) is a subspace of $H_0(\mathrm{div}, \Omega)$:

$$X = \{\mathbf{u} \in H_0(\mathrm{div}, \Omega) \mid \boldsymbol{\nabla} \cdot \mathbf{u} = 0 \text{ in } \Omega\}.$$

With the inner product (5) we can define the space $X^\perp$ by

$$X^\perp = \left\{ \mathbf{u} \in H_0(\mathrm{div}, \Omega) \;\middle|\; (\mathbf{u}, \mathbf{v})_{H(\mathrm{div},\Omega)} = 0,\ \forall \mathbf{v} \in X \right\}.$$

The space X and $X^\perp$ allow us to decompose each element in $\mathbf{u} \in H_0(\mathrm{div}, \Omega)$ uniquely as

$$\mathbf{u} = \mathbf{u}_X + \mathbf{u}_{X^\perp}, \quad \mathbf{u}_X \in X, \quad \mathbf{u}_{X^\perp} \in X^\perp.$$

The divergence operator is a surjective map from $H_0(\mathrm{div}, \Omega)$ onto $L^2_0(\Omega)$ and it is a bijection from $X^\perp$ to $L^2_0(\Omega)$ (see [11, Corollary 2.4]). This means that, for each $\mathbf{w} \in H_0(\mathrm{div}, \Omega)$, there exists a unique $\mathbf{v} \in X^\perp$ such that $\mathrm{div}\, \mathbf{v} = \mathrm{div}\, \mathbf{w} \in L^2_0(\Omega)$. In particular, div^{-1} is a well-defined continuous map from $L^2_0(\Omega)$ to $X^\perp$ and we have the Poincaré inequality [4, p.302]

$$\|\mathbf{v}\|_{H(\mathrm{div},\Omega)} \leq c_P \, \|\mathrm{div}\, \mathbf{v}\|_{L^2(\Omega)},$$

where c_P is independent of $\mathbf{v}$. This implies that, if we have a set of linearly independent functions $\{q_1, \ldots, q_n\} \in L^2_0(\Omega)$, then there exist unique vectors $\mathbf{v}_i \in X^\perp$ with $\mathrm{div}\, \mathbf{v}_i = q_i$ and these vectors $\mathbf{v}_i$ are linearly independent in $X^\perp$ and therefore also in $H_0(\mathrm{div}, \Omega)$. The converse only holds for $X^\perp$. Indeed, if $\mathbf{u}$ and $\mathbf{v}$ are linearly independent in $X^\perp$, then $\mathrm{div}\, \mathbf{u}$ and $\mathrm{div}\, \mathbf{v}$ are linearly independent in $L^2_0(\Omega)$. The generalization for $\mathbf{u}, \mathbf{v} \in H_0(\mathrm{div}, \Omega)$ is generally not true: Let $S = \{\mathbf{v}_1, \ldots, \mathbf{v}_n\}$ be a set of linear independent vectors in $H_0(\mathrm{div}, \Omega)$ with $\mathrm{div}\, \mathbf{v}_i \neq 0$ and let $\mathrm{rank}(\mathrm{div}\, \mathbf{v}_1, \ldots, \mathrm{div}\, \mathbf{v}_n) = k$, then we can select k vectors from the set S which form a basis for a k-dimensional subspace of $X^\perp$.

This last result is the keystone to ensure that it is always possible to reduce into a square and invertible sub-part, the algebraic system resulting from any stable discretization of the constraint.

3.1. Variational formulation and its discretization

The variational formulation of problem (1) writes: *Find* $\mathbf{u}_\psi \in X$ *such that*

$$\int_\Omega \mathbf{u}_\psi \cdot \mathbf{v} \, d\mathbf{x} = \int_\Omega \mathbf{u} \cdot \mathbf{v} \, d\mathbf{x}, \quad \forall \mathbf{v} \in X. \tag{6}$$

Due to the nature of X, $\mathbf{u}_\phi$ and $\mathbf{u}_H$ disappear.

We firstly introduce the Raviart-Thomas space [18]

$$R_p = \left(\mathbb{P}^0_p(\Lambda) \otimes \mathbb{P}_{p-1}(\Lambda)\right) \times \left(\mathbb{P}_{p-1}(\Lambda) \otimes \mathbb{P}^0_p(\Lambda)\right), \tag{7}$$

where $\mathbb{P}_N(\Lambda)$ is the space of polynomials with degree $\leq N$ and $\mathbb{P}^0_p(\Lambda)$ denotes the space of polynomials of degree p vanishing on ± 1. The dimension of R_p is equal to $2(p-1)p$.

The solution is approximated by $\mathbf{u}_{\psi,p} = (u^x_{\psi,p}, u^y_{\psi,p})$ in R_p with

$$u^x_{\psi,p}(x,y) = \sum_{i=1}^{p-1}\sum_{j=1}^{p} u^x_{\psi,p}(\xi_i,\zeta_j)\, h_i(x)\, \tilde{h}_j(y),$$
$$u^y_{\psi,p}(x,y) = \sum_{i=1}^{p}\sum_{j=1}^{p-1} u^y_{\psi,p}(\zeta_i,\xi_j)\, \tilde{h}_i(x)\, h_j(y).$$

Let $\Sigma_{GLL} = \{(\xi_i, \rho_i) \mid 0 \le i \le N\}$ and $\Sigma_{GL} = \{(\zeta_i, \omega_i) \mid 1 \le i \le N\}$ denote respectively the sets of Gauss-Lobatto-Legendre and Gauss-Legendre quadrature nodes and weights (see [10]). Likewise, $h_i(x) \in \mathbb{P}_N(\Lambda)$ and $\widetilde{h}_j(x) \in \mathbb{P}_{N-1}(\Lambda)$ are respectively the canonical Lagrange polynomial interpolation basis built on Σ_{GLL} and on Σ_{GL}.

With this choice, the divergence of $\mathbf{u}_{\psi,p}$ is a polynomial of degree $p-1$. Consequently, if the divergence is orthogonal to all polynomial of $\mathbb{P}_{p-1}(\Omega)$, it is necessarily equal to 0. This point gives a new characterization for $X_p = R_p \cap X$:

$$X_p = \left\{ \mathbf{u}_{\psi,p} \in R_p \;\middle|\; \frac{\partial u^x_{\psi,p}}{\partial x} + \frac{\partial u^y_{\psi,p}}{\partial y} = 0 \right\},$$
$$X_p = \left\{ \mathbf{u}_{\psi,p} \in R_p \;\middle|\; \int_\Omega \left(\frac{\partial u^x_{\psi,p}}{\partial x} + \frac{\partial u^y_{\psi,p}}{\partial y} \right) q \, d\mathbf{x} = 0,\ \forall q \in \mathbb{P}_{p-1}(\Omega) \right\}.$$

3.2. A basis for X_p

The first step consists in determining the dimension of the space X_p, that we denote by N_1:

$$N_1 = \dim R_p - N_2 = 2(p-1)p - N_2,$$

where N_2 is the dimension of the range of the divergence operator which is also the dimension of $P_{p-1}(\Omega) \cap L^2_0(\Omega)$ and then equals to $p^2 - 1$. We deduce that $N_1 = (p-1)^2$.

Remark 1. One can also view N_2 as the number of necessary and sufficient equations to ensure $\nabla \cdot \mathbf{u}_{\psi,p} \equiv 0$:

$$\nabla \cdot \mathbf{u}_{\psi,p} \in \mathbb{P}_{p-1}(\Omega) \quad \text{so} \quad N_2 \le p^2.$$

Due to the boundary conditions (here $\mathbf{u}_{\psi,p} \cdot \mathbf{n} = 0$ on $\partial\Omega$), there is a dependent equation in the two dimensional case [5], since

$$\int_\Omega \nabla \cdot \mathbf{u}_{\psi,p} L_0(x) L_0(y) d\mathbf{x} = 0,\ \forall \mathbf{u}_{\psi,p} \in R_p.$$

Indeed, the polynomial $L_0(x)L_0(y)$ is a spurious mode and it reduces the number of independent equations from p^2 to $p^2 - 1$. Consequently, we require $N_2 = p^2 - 1$ test functions q to ensure $\int_\Omega \nabla \cdot \mathbf{u}_{\psi,p}\, q \, d\mathbf{x} = 0$.

Once the dimension is known, we describe now how to proceed to derive a divergence free basis from any N_1 given vectors of R_p

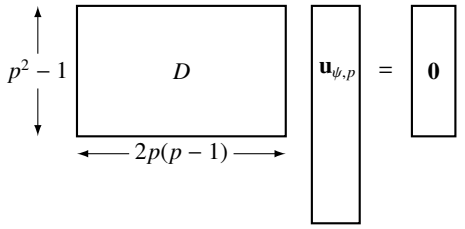

Figure 1: Algebraic system.

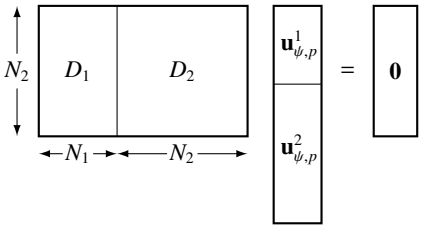

Figure 2: Decomposition of D.

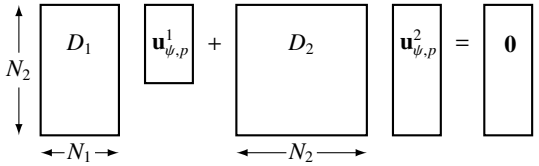

Figure 3: Algebraic system.

3.2.1. Algebraic characterization of X_p

Let $\mathbf{u}_{\psi,p}$ be in X_p. The divergence of $\mathbf{u}_{\psi,p}$ is orthogonal to p^2-1 polynomials of degree $p-1$. It is equivalent to saying that the divergence of $\mathbf{u}_{\psi,p}$ nullifies into p^2-1 Gauss points. The algebraic divergence equation writes $D\,\mathbf{u}_{\psi,p} = \mathbf{0}$, where D is a rectangular matrix with p^2-1 rows and $2p(p-1)$ columns (see Figure 1).

One splits D into $D_1 \oplus D_2$ and $\mathbf{u}_{\psi,p}$ into $\mathbf{u}^1_{\psi,p} \oplus \mathbf{u}^2_{\psi,p}$. The vector $\mathbf{u}^1_{\psi,p}$ contains $N_1 = (p-1)^2$ values of $\mathbf{u}_{\psi,p}$, whereas $\mathbf{u}^2_{\psi,p}$ contains the $N_2 = p^2-1$ remaining values (see Figure 2). The equation $D\,\mathbf{u}_{\psi,p} = \mathbf{0}$ becomes $D_1\,\mathbf{u}^1_{\psi,p} + D_2\,\mathbf{u}^2_{\psi,p} = \mathbf{0}$, as shown in Figure 3.

Since, the p^2-1 rows of D are independent, there exists at least one choice of matrix D_2 invertible and the system leads to a relation between $\mathbf{u}^2_{\psi,p}$ and $\mathbf{u}^1_{\psi,p}$:

$$\mathbf{u}^2_{\psi,p} = -D_2^{-1} D_1 \mathbf{u}^1_{\psi,p}. \tag{8}$$

This equation is very important since it means that, if we have any part $\mathbf{u}^1_{\psi,p}$ of $\mathbf{u}_{\psi,p}$, we can build the complementary $\mathbf{u}^2_{\psi,p}$ such that divergence of $\mathbf{u}_{\psi,p}$ equals 0. This argument allows us to build a basis of X_p.

3.2.2. Basis of X_p

The technique we use to project any vector of R_p on X_p is in the spirit of that published in [2] and used to solve the Stokes problem.

We consider $\mathbf{v}_p \in R_p$. Our strategy consists in combining implicitly:

- A reduction from $\mathbf{v}_p$ to $\mathbf{v}^1_p$.
- An extension from $\mathbf{v}^1_p$ to $\mathbf{w}_p = (\mathbf{v}^1_p, \mathbf{v}^2_p)$ such that $\nabla\cdot\mathbf{w}_p = 0$ ensured by the multiplication

of $\mathbf{v}_p^1$ by the matrix

$$M = \begin{bmatrix} I_{N_1} \\ -D_2^{-1} D_1 \end{bmatrix}.$$

The first block of M is the identity matrix of order N_1. The second block contains N_2 rows and N_1 columns. It ensures the passage from $\mathbf{v}_p^1$ to $\mathbf{v}_p^2$.

- For each $\mathbf{v}_p \in R_p$ one associates a vector $\mathbf{w}_p$ of X_p.

By consequent, our strategy for the construction of a basis of X_p consists in:

- Choosing $N_1 = (p-1)^2$ vectors $(\mathbf{v}_p^k)_{k=1..N_1}$ of the basis of R_p.
- For each one of these N_1 vectors, we consider its N_1-size reduced part denoted by $\mathbf{v}_p^{k,1}$.
- We carry out the divergence-free extension $(\mathbf{w}_p^k)_{k=1..N_1} = (M\,\mathbf{v}_p^{k,1})_{k=1..N_1}$.

The $(\mathbf{w}_p^k)_{k=1..N_1}$ family is a basis of X_p. Consequently, $\mathbf{u}_{\psi,p} \in X_p$ can be decomposed according to $\mathbf{u}_{\psi,p} = \sum_{k=1}^{N_1} \alpha_k \mathbf{w}_p^k$ and the discrete variational formulation similar to (6) writes: *Find* $\mathbf{u}_{\psi,p} \in X_p$ *such that*

$$\sum_{k=1}^{N_1} (\mathbf{w}_p^k, \mathbf{w}_p^i)_p \alpha_k = (\mathbf{u}_p, \mathbf{w}_p^i)_p.$$

This can be written as

$$\underline{\mathcal{M}}\,\underline{\boldsymbol{\alpha}} = \underline{\mathcal{F}},$$

with, for $1 \le i, k \le N_1$,

$$\underline{\mathcal{M}}_{ik} = (\mathbf{w}_p^k, \mathbf{w}_p^i)_p,$$
$$\underline{\mathcal{F}}_k = (\mathbf{u}, \mathbf{w}_p^k)_p.$$

Finally, this system is equivalent to

$$M^T B M\,\mathbf{u}_{\psi,p}^1 = M^T B\,\mathbf{u}_p,$$

where B refers to the classical mass matrix computed using the $(h_i \times \tilde{h}_j) \otimes (\tilde{h}_i \times h_j)$ basis.

§4. Computation of the irrotational component

A similar strategy to that described previously is used to compute the irrotational component $\mathbf{u}_\phi$, so we will limit to the description of the outline and we will not give all the details of its implementation.

Firstly, we introduce three spaces of functions:

$$H(\mathrm{rot}, \Omega) = \left\{ \mathbf{w} \in (L^2(\Omega))^2 \;\middle|\; \nabla \times \mathbf{w} \in L^2(\Omega) \right\},$$
$$H_0(\mathrm{rot}, \Omega) = \{ \mathbf{w} \in H(\mathrm{rot}, \Omega) \mid \mathbf{w} \times \mathbf{n} = 0 \text{ on } \partial\Omega \},$$
$$Y = \{ \mathbf{u} \in H_0(\mathrm{rot}, \Omega) \mid \nabla \times \mathbf{u} = 0 \text{ in } \Omega \}.$$

The variational formulation of Problem (1) writes: *Find* $\mathbf{u}_\phi \in Y$ *such that*

$$\int_\Omega \mathbf{u}_\phi \cdot \mathbf{v}\, d\mathbf{x} = \int_\Omega \mathbf{u} \cdot \mathbf{v}\, d\mathbf{x}, \quad \forall \mathbf{v} \in Y.$$

For the discretization, we introduce the Nédélec space [15]

$$N_p = (\mathbb{P}_{p-1}(\Lambda) \otimes \mathbb{P}^0_p(\Lambda)) \times (\mathbb{P}^0_p(\Lambda) \otimes \mathbb{P}_{p-1}(\Lambda)).$$

The solution is approximated by $\mathbf{u}_{\phi,p} = (u^x_{\phi,p}, u^y_{\phi,p}) \in Y_p = N_p \cap Y$ with

$$u^x_{\phi,p}(x,y) = \sum_{i=1}^{p} \sum_{j=1}^{p-1} u^x_{\phi,p}(\zeta_i, \xi_j)\, \tilde{h}_i(x)\, h_j(y),$$

$$u^y_{\phi,p}(x,y) = \sum_{i=1}^{p-1} \sum_{j=1}^{p} u^y_{\phi,p}(\xi_i, \zeta_j)\, h_i(x)\, \tilde{h}_j(y).$$

As previously, we build a basis of Y_p. With the same reasoning as for X_p and taking into account the same spurious mode $L_0(x)L_0(y)$, we determine the size of Y_p equal to $N_1 = (p-1)^2$.

Then the constraint $\nabla \times \mathbf{u}_{\phi,p} = \mathbf{0}$ is written into $N_1 = (p-1)^2$ Gauss points and gives an algebraic equations $R\mathbf{u}_{\phi,p} = \mathbf{0}$. A splitting strategy for the matrix R into $R_1 \oplus R_2$ and the vector $\mathbf{u}_{\phi,p}$ into $\mathbf{u}^1_{\phi,p} \oplus \mathbf{u}^2_{\phi,p}$ gives $R_1\mathbf{u}^1_{\phi,p} + R_2\mathbf{u}^2_{\phi,p} = \mathbf{0}$ and finally $\mathbf{u}^2_{\phi,p} = -R_2^{-1}R_1\mathbf{u}^1_{\phi,p}$.

Thanks to the $(N_1 + N_2) \times N_1$ matrix

$$N = \begin{bmatrix} I_{N_1} \\ -R_2^{-1}R_1 \end{bmatrix},$$

we can construct a basis of Y_p.

Finally we obtain the system $N^T \tilde{B} N\, \mathbf{u}^1_{\phi,p} = N^T \tilde{B}\, \mathbf{u}_p$, where $\tilde{B}$ refers to the classical mass matrix computed using $(\tilde{h}_i \times h_j) \otimes (h_i \times \tilde{h}_j)$ basis.

§5. Numerical results

To illustrate the efficiency of our approach for the Hodge Helmholtz decomposition, we have made a numerical experiment in the square $\Omega = (-1,+1)^2$ with the case $\mathbf{u} = \mathbf{u}_\psi + \mathbf{u}_\phi + \mathbf{u}_H$ corresponding to the following components:

$$\begin{aligned} \mathbf{u}_\psi &= (\sin(\pi x)\cos(\pi y), -\sin(\pi y)\cos(\pi x)), \\ \mathbf{u}_\phi &= (\sin(\pi y)\cos(\pi x), \sin(\pi x)\cos(\pi y)), \\ \mathbf{u}_H &= (0.5, -1). \end{aligned}$$

The component $\mathbf{u}_{\psi,p}$ is approximated as outlined in Section 3, while the irrotational part $\mathbf{u}_{\phi,p}$ is computed as outlined in Section 4. Finally, $\mathbf{u}_H$ is calculated by the relation $\mathbf{u}_H = \mathbf{u} - \mathbf{u}_\psi - \mathbf{u}_\phi$.

Table 1 gives $\|\nabla \cdot \mathbf{u}_{\psi,p}\|_{L^2(\Omega)}$ and $\|\nabla \times \mathbf{u}_{\phi,p}\|_{L^2(\Omega)}$ as a function of the polynomial degree p. As expected, the norms remain close to round-off *independently* of p.

Figure 4 exhibits on a semi-logarithmic scale the $(L^2(\Omega))^2$-norm of the error for the three components as a function of the polynomial degree p. We can observe a spectral decrease.

Figure 5 displays the Hodge Helmholtz decomposition of the vector $\mathbf{u}$.

p	4	8	12	16
$\|\|\nabla \cdot \mathbf{u}_{\psi,p}\|\|_{L^2(\Omega)}$	8.56×10^{-16}	1.71×10^{-15}	1.95×10^{-15}	5.23×10^{-15}
$\|\|\nabla \times \mathbf{u}_{\phi,p}\|\|_{L^2(\Omega)}$	4.90×10^{-16}	2.18×10^{-15}	3.87×10^{-15}	5.09×10^{-15}

Table 1: $L^2(\Omega)$-norm of the divergence and the rotational of solenoidal and irrotational components.

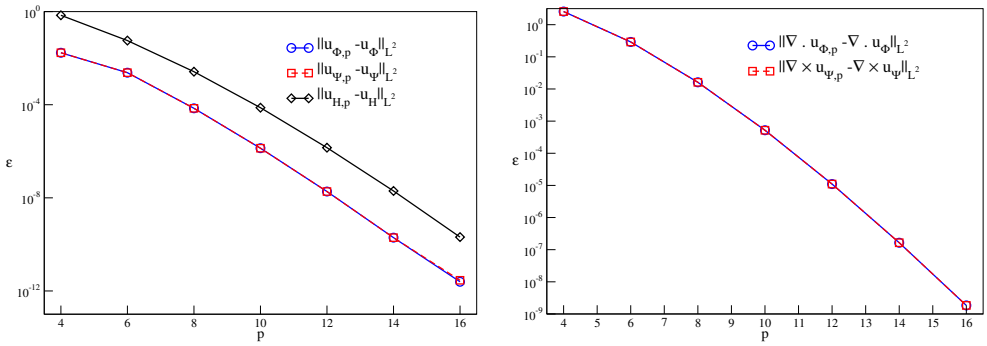

Figure 4: $(L^2(\Omega))^2$-norm of the error as a function of the polynomial degree p.

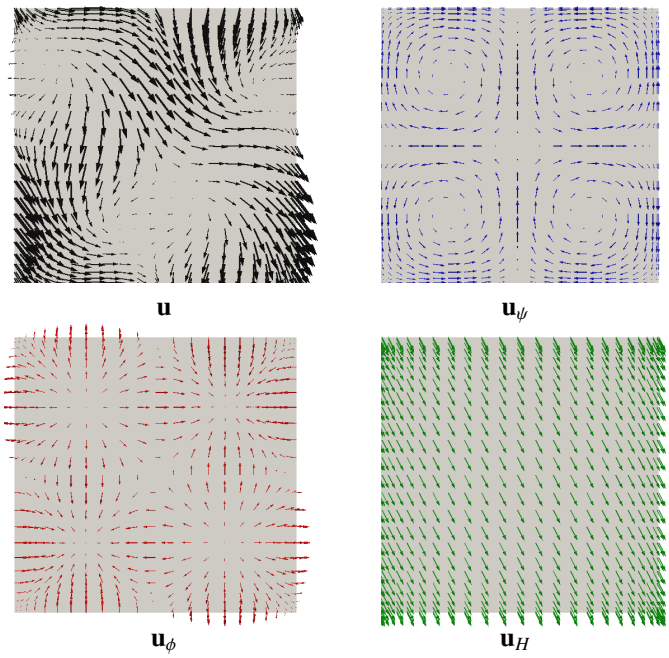

Figure 5: Decomposition of the vector and its three components.

References

[1] Ahusborde, E., Azaïez, M., Deville, M., and Mund, E. Constructive spectral approaches for the Helmholtz decomposition of a vector field. *Applied Numerical Mathematics 58* (2008), 955–967.

[2] Ahusborde, E., Gruber, R., Azaïez, M., and Sawley, M. Physics-conforming constraints-oriented numerical method. *Physical Review E 75* (2007).

[3] Arnold, D., and Falk, R. A uniformly accurate finite element method for the Reissner-Mindlin plate. *SIAM J. Numer. Anal. 26* (1989), 1276–1290.

[4] Arnold, D., Falk, R., and Winther, R. Finite element exterior calculus: from Hodge theory to numerical stability. *Bull. Amer. Math. Soc. 47* (2010), 281–354.

[5] Azaiez, M., Bernardi, C., and Grundmann, M. Spectral methods applied to porous media equations. *East-West Journal of Numerical Mathematics 2* (1994), 91–105.

[6] Batchelor, G. *An Introduction to Fluid Dynamics*. Cambridge University Press, Cambridge, 1967.

[7] Brezzi, F., and Fortin, M. Numerical approximations of Mindlin-Reissner plates. *Math. Comp. 47* (1986), 151–158.

[8] Caltagirone, J., and Breil, J. Sur une méthode de projection vectorielle pour la résolution des équations de Navier-Stokes. *C.R. Acad. Sci. Paris 327* (1999), 1179–1184.

[9] Chorin, A. Numerical solution of the Navier-Stokes equations. *Math. Comput. 22* (1968), 745–762.

[10] Deville, M., Fischer, P., and Mund, E. *High-Order Methods for Incompressible Fluid Flow*. Cambridge University Press, Cambridge, 2002.

[11] Girault, V., and Raviart, P. *Finite Element Methods for Navier-Stokes Equations*. Series in Computational Mathematics. Springer-Verlag, Berlin, 1986.

[12] Goda, K. A multistep technique with implicit difference schemes for calculating two and three dimensional cavity flows. *J. Comput. Physics 30* (1979), 76–95.

[13] Harouna, S., and Perrier, V. Helmholtz Hodge decomposition on $[0, 1]^d$ by divergence-free and curl-free wavelets. *Lecture Notes in Computer Science 6920* (2012), 311–329.

[14] Morse, P., and Feshbach, H. *Methods of Theoretical Physics*. McGraw-Hill, New York, 1953.

[15] Nédélec, J. Mixed finite elements in $\mathbb{R}^3$. *Numerishe Mathematik 35* (1980), 315–341.

[16] Palit, B., Basu, A., and Mandal, M. Applications of the discrete Hodge Helmholtz decomposition to image and video processing. *Lecture Notes in Computer Science 3776* (2005), 497–505.

[17] Petronetto, F., Paiva, A., Lage, M., Tavares, G., Lopes, H., and Lewiner, T. Meshless Helmholtz Hodge decomposition. *IEEE Transaction on Visualization and Computer Graphics 16* (2010), 338–342.

[18] Raviart, P., and Thomas, J. A mixed finite element method for second order elliptic problems. *Mathematical Aspects of Finite Element Method. Lecture Notes in Mathematics 606* (1977), 292–315.

[19] Témam, R. Sur l'approximation de la solution de Navier-Stokes par la méthode des pas fractionnaires I, II. *Arch. Rat. Mech. Anal 32* (1969), 135–153, 377–385.

Etienne Ahusborde
University of Pau. LMAP UMR 5142 CNRS.
etienne.ahusborde@univ-pau.fr

Mejdi Azaïez
University of Bordeaux. IPB-I2M UMR 5295.
azaiez@ipb.fr

Jean-Paul Caltagirone
University of Bordeaux. IPB-I2M UMR 5295.
calta@ipb.fr

Mark Gerritsma
Department of Aerospace Engineering,
TU Delft, The Netherlands.
M.I.Gerritsma@tudelft.nl

Antoine Lemoine
University of Bordeaux. IPB-I2M UMR 5295.
antoine.lemoine@ipb.fr